Spin polarization of the Ar^{*} $2p^{-1}_{1/2}$ 4s, and $2p^{-1}_{1/2}$ 3d resonant Auger decay

G. Turri[1,2,*], B. Lohmann[3,4], B. Langer[5], G. Snell[1], U. Becker[4], and N. Berrah[1]

[1]*Department of Physics, Western Michigan University, Kalamazoo, Michigan 49008, USA*
[2] *Lawrence Berkeley National Laboratory, Berkeley, CA, USA.*
[3]*Institut für Theoretische Physik, Westfälische Wilhelms-Universität Münster, Wilhelm-Klemm-Strasse 9, D-48149 Münster, Germany*
[4]*Fritz-Haber-Institut der Max-Planck-Gesellschaft, Faradayweg 4-6, D-14195 Berlin/Dahlem, Germany*
[5]*Max-Born-Institut für Nichtlineare Optik und Kurzzeitspektroskopie, Max-Born-Strasse 2A, D-12489 Berlin, Germany*

[*] *Present address: CREOL the College of Optics and Photonics, University of Central Florid, Orlando, FL, USA.*

Introduction

It is well known that electrons photoemission by either normal or resonant Auger decay, can be spin polarized[1-8]. As for the electrons emitted by direct photoionization, the spin polarization is caused by the spin-orbit interaction either in the atom or in the continuum, and the two different mechanisms of transferred spin polarization (TSP)[1-8] and dynamic spin polarization (DSP)[6,7] can be distinguished. TSP occurs because of the intrinsic polarization of the incoming photon, which generates an asymmetric sublevel population in the atom which is eventually transferred to the emitted Auger electrons, while the DSP is generated dynamically, i.e. by relativistic or spin-orbit effects during the Auger emission, and therefore requires no intrinsic spin polarization. In general, DSP in atoms vanishes when measurements integrate the emission angle of the electrons, whereas TSP can still be non-zero. Also, there may be intrinsic reasons for small or vanishing DSP in an atom showing high TSP as was shown for the case of the Auger decay from the $2p^{-1}$ excited state of Ar, [8]. A high TSP is expected, and was measured for the $2p^{-1}4s$ state, due to the close similarity of the Auger decay of the resonantly excited 2p state with the direct photoionization of a *d* shell. A low DSP results from the fact that electrons are emitted with partial waves with equal orbital angular momentum, thus resulting in small phase difference in the continuum. In general it is also believed that DSP should vanish when the fine structure of the LS multiplet is not resolved. In our previous work [8] we showed that the last statement is not necessarily

true, and that some small DSP can still be observed also in the case of partially unresolved fine structure, due to strong configuration interaction.

In the present work, we extend our former investigation to the Auger decay of the $2p^{-1}3d$ excited state in argon. As compared to the $2p_{1/2}^{-1}4s$ state that mainly decays to final $3p^4$ nl states of binding energy between 32 and 38 eV, the most intense transitions from the $2p_{1/2}^{-1}3d$ are to states between 37 and 41 eV binding energy. Also, some states in the 32 - 38 eV range can be more efficiently populated from the $2p_{1/2}^{-1}3d$ than from the $2p_{1/2}^{-1}4s$ excited state [9]. The experimental results will be compared with calculations based on the relativistic distorted wave approximation technique described in our previous paper [8], using the same type of wavefunctions for the initial, intermediate and final state opportunely modified for the $2p^{-1}3d$ case (36 CFS-CI calculation). In addition, our previous investigation of the $2p^{-1}4s$ decay will be extended to a broader energy range with new measurements.

Experimental method

The experimental apparatus has been described elesewhere [8, 10], thus only a brief description will be given here. Measurements were performed at the beamline 4.0.2 at the advanced light source (ALS) at Lawrence Berkeley National Laboratory in Berkeley, CA. The Eliptically Polarized Undulator (EPU) was set to deliver either linearly or circularly polarized light (polarization 100% in both cases). Auger electrons were collected in a plane perpendicular to the photon propagation direction and at 45 deg with respect to the plane of the storage ring. Their kinetic energy was measured by time-of-flight (TOF) detectors [10]. A Mott detector of the Rice type [11, 12], operated at 25 KV, S_{eff} = 0.13 +/- 0.02, mounted after the drift tube of the TOF detector, measured the spin polarization along the photon propagation axis. Geometrical asymmetries of the apparatus were accounted for, by the standard technique of reversing the helicity of the photons when using circularly polarized light and rotating by 90° the polarization of linearly polarized light. With this geometry, the TSP and DSP take simple forms [10-and references therein]:

$$P_{trans} = \frac{2\sqrt{3}\hat{\imath}_1}{2\sqrt{2} - \acute{a}_2} \qquad (1)$$

$$P_{din} = \frac{6\hat{\imath}_2}{2\sqrt{2} - \acute{a}_2} \qquad (2)$$

Formulas (1) and (2) are derived within the two-step model [1, 13], where the excitation and the Auger decay are treated independently. Because the first step produces an excited atom created with maximum alignment and because of the chosen geometry, the first step excitation only contributes constants terms. The α_2 , ξ_1 and ξ_2 are combinations of the matrix elements and phases of the second step Auger decay only. α_2 is the intrinsic Auger anisotropy parameter and ξ_1 and ξ_2 are called the transferred and the dynamic spin polarization parameters respectively.

Results and discussion

In figure 1, the spin-unresolved spectrum (average of spin-up and spin-down spectra) of the $2p_{1/2}^{-1}$ 3d Auger decay measured with circularly polarized light is displayed. It consists of some fifteen peaks, where every peak is a manifold of many overlapping components, corresponding to the transitions to the different final states of the singly-ionized argon atom. The correct assignment of the peaks is not straightforward, especially for time of flight measurements, where some small error in the kinetic energy axis is to be expected. The number of the Ar^+ states their binding energy and the relative intensities of the Auger transitions from the Ar $2p_{1/2}^{-1}$ 3d state are known from [9]. The angular distribution has been measured for a few transitions only [14] and the spin polarization has never been measured. From Mursu's [9] and Langer's [14] values, we were able to identify the components of all the peaks, and we report them in table 1 (very weak transitions have been neglected). We are labeling the peaks consistently with our previous publication [8], starting from the most bound one around 33.5 eV binding energy. For a more quantitative comparison, we used a best-fit method where we

imposed the relative energy and the relative intensity of each manifold components to be equal to Mursu's values [9], and we allowed rigid shifts of the manifolds position to fit our experimental data. To account for the effects of the unknown angular distributions, we further assumed that all the components of each manifold have similar anisotropy parameters and simply rescaled the manifold overall intensity to fit our experimental data. The results are the dashed and continuous curves in figure 1.

Figures 2 and 3 depict the spin resolved spectra for TSP and DSP respectively. Because of the complex structure of the manifolds, we did not try to separate their components in the spin-resolved experimental spectra, nor did we fit each manifold with some properly chosen analytical function. Rather, we took the manifold areas and used them to obtain the spin polarization, assuming that the peak broadening due to finite instrumental resolution does not significantly contribute to the overall area of the manifold. The results are reported in columns four and five of table 1. For the sign of the polarization, we are adopting the same notation as our previous paper [8], where a positive spin polarization indicates that the electron is emitted preferentially with the spin parallel, rather than anti-parallel, to the photon propagation direction. The errors in table 1 account for both the statistical error (evaluated from the manifold areas) and the indetermination of the Sherman function. Also, we performed the same analysis for the newly collected spectra of the Auger decay of the Ar $2p_{1/2}^{-1}$ 4s state and reported the results in columns 6 and 7 of tab.1. The latter show reasonable agreement with our previous measurement for peaks 1 to 4, they have larger errors due to a lower statistic of the new measurements. In general, TSP is stronger for the decay of the $2p_{1/2}^{-1}$ 4s than $2p_{1/2}^{-1}$ 3d. On the contrary, the $2p_{1/2}^{-1}$ 3d state shows significant amount of DSP for peaks 2c, 11 and 13. Peak 12 in figure 3 suggests that its components have strong DSP, though the total polarization vanishes when the manifold is not resolved. Also, peaks 11 and the unresolved 8-9 show similar values of DSP in the $2p_{1/2}^{-1}$ 4s and $2p_{1/2}^{-1}$ 3d decay.

The results of the 36 CSF-CI calculations for the $2p_{1/2}^{-1}$ 3d state are compared to the TSP and DSP we measured in the 33.5 - 37 eV binding energy range in figures 4 and 5 respectively. The calculations reproduce correctly the DSP, with the only exception of peak 2c for which we assume negligible polarization. On the contrary, they strongly overestimate the TSP of peak 5, and they find the wrong sign of the polarization of peak

3. The non complete agreement between calculation and theory would suggest that for the $2p_{1/2}^{-1}$ 3d state it is the TSD, rather than the DSP as we showed for the $2p_{1/2}^{-1}$ 4s [8], to be more sensitive to the calculation details. To test this hypothesis, an extended approach, including a larger basis sets than the 36 CSF-CI, should be tempted, which is beyond the present scope of this paper.

In conclusion, we showed that the DSP already observed in the Auger decay of the $2p_{1/2}^{-1}$ 4s, is also observable, if not stronger, in the Auger decay of the $2p_{1/2}^{-1}$ 3d state at medium energy resolution. For the latter state, an interpretation of the DSP as configuration interaction induced effect in the final ionic state only brings partial agreement within a 36 basis configuration state functions calculation.

Experimental work at the ALS was funded by the U.S. DOE, Office of Science, BES, Divisions of Chemical, Biosciences,and Geophysical Sciences. We are thankful to J. Bozek and A. Young for their help in the measurements at the beamline.

References

[1] N.M. Kabachnik et al., J. Phys. B **21**, 3695 (1988)
[2] B. Lohmann et al., J. Phys. B **26**, 3327 (1993)
[3] G. Snell et al., Phys. Rev. Lett. **76**, 3923 (1996).
[4] G. Snell et al., Phys. Rev. Lett. **82**, 2480 (1999).
[5] U. Hergenhahn et al., Phys. Rev. Lett. **82**, 5020 (1999).
[6] U. Hergenhahn, et al., Phys. Rev. Lett. **82**, 5020 (1999).
[7] B. Lohmann, J. Phys. B **32**, L643 (1999).
[8] B. Lohmann et al., Phys. Rev. A **71**, 020701 (2005).
[9] J. Mursu et al., J. Phys. B **29**, 4387 (1996).
[10] G. Snell et al., Phys. Rev. A **66**, 022701 (2002).
[11] G..C. Burnett et al., Rev. Sci. Instrum. **65**, 1893 (1994).
[12] G.. Snell et al., Rev. Sci. Instrum. **71**, 2608 (2000).
[13] W. Mehlhorn, in *X-ray and Inner Shell Processes*, edited by T.A. Carlson, M. O. Krause, and S. T. Manson, AIP Conf. Proc. No. 215 sAIP, New York, 1990d, p. 465.
[14] B. Langer et al., J. Phys. B **30**, 4255 (1997).

Peak	Final State	Binding Energy [eV]	Ar $2p_{1/2}3d$ Transferred Polarization	Ar $2p_{1/2}3d$ Dynamic Polarization	Ar $2p_{1/2}4s$ Transferred Polarization	Ar $2p_{1/2}4s$ Dynamic Polarization
1	$3p^4(^3P)3d\ ^4F_{3/2,5/2}$	33.50	- 0.14 (+/- 0.2)	+ 0.2 (+/- 0.3)	- 0.05 (+/- 0.06)	+ 0.03 (+/- 0.03)
2 a-b	$3p^4(^3P)3d\ ^4P$	34.05	+ 0.25 (+/- 0.15)	- 0.1 (+/- 0.2)	- 0.36 (+/- 0.06)	+ 0.03 (+/- 0.03)
2 c	$3p^4(^1D)3d\ ^2G_{9/2}$	34.88	+ 0.13 (+/- 0.25)	+ 0.7 (+/- 0.4)	-	-
3	$3p^4(^1D)3d\ ^2F_{5/2}$	36.00	+ 0.33 (+/- 0.2)	- 0.15 (+/- 0.2)	-	-
4	$3p^4(^1S)4s\ ^2S_{1/2}$	36.50	-	-	- 0.8 (+/- 0.2)	- 0.06 (+/- 0.07)
5	$3p^4(^1D)3d\ ^2D_{5/2}$ $3p^4(^1D)3d\ ^2D_{3/2}$	37.13 37.19	+ 0.1 (+/- 0.05)	+ 0.06 (+/- 0.09)	- 0.36 (+/- 0.2)	- 0.35 (+/- 0.1)
6	$3p^4(^1D)3d\ ^2P_{3/2}$ $3p^4(^1D)3d\ ^2P_{1/2}$	37.38 37.44				
7	$3p^4(^1S)3d\ ^2D_{5/2}$ $3p^4(^1S)3d\ ^2D_{3/2}$	38.03 38.07	+ 0.3 (+/- 0.1)	- 0.03 (+/- 0.2)	-	-
8	$3p^4(^3P)5s\ ^2P_{1/2}$ $3p^4(^3P)4d\ ^4D_{5/2}$ $3p^4(^3P)4d\ ^4D_{3/2}$ $3p^4(^1D)3d\ ^2S_{1/2}$	38.46 38.55 38.57 38.59	+ 0.01 (+/- 0.05)	+ 0.11 (+/- 0.09)	+ 0.11 (+/- 0.2)	+ 0.19 (+/- 0.13)
9	$3p^4(^3P)4d\ ^4F_{5/2}$ $3p^4(^3P)4d\ ^4F_{3/2}$ $3p^4(^3P)4d\ ^4P_{3/2}$	38.83 38.86 38.88				
10	- $3p^4(^3P)4d\ ^2P_{1/2,3/2}$ $3p^4(^3P)4d\ ^2D_{5/2}$ $3p^4(^3P)4d\ ^2D_{3/2}$	39.24 39.31 39.63 39.65	- 0.18 (+/- 0.15)	+ 0.05 (+/- 0.2)	-	-
11	$3p^4(^1D)5s\ ^2D_{5/2}$ $3p^4(^3P)4f\ J=3/2$	40.04 40.07	- 0.3 (+/- 0.2)	+ 0.45 (+/- 0.2)	+ 0.45 (+/- 0.4)	+ 0.56 (+/- 0.3)
12	$3p^4(^3P)6s\ ^4P_{5/2}$ $3p^4(^1D)4d\ ^2D_{5/2}$ $3p^4(^1D)4d\ ^2F_{5/2}$ $3p^4(^3P)6s\ ^2P_{1/2}$	40.41 40.52 40.59 40.63	+ 0.18 (+/- 0.07)	+ 0.05 (+/- 0.1)	-	-

	$3p^4(^3P)5d\ ^4P_{3/2}$ $3p^4(^3P)5d\ ^4P_{5/2}$	40.72 40.78				
13	$3p^4(^3P)5d\ ^2D_{3/2}$ $3p^4(^3P)5d\ ^2P_{1/2}$	41.10 41.12	+ 0.21 (+/- 0.2)	+ 0.4 (+/- 0.2)	-	-
14	$3p^4(^3P)6d\ ^4P_{1/2}$	41.61	- 0.12 (+/- 0.2)	0 (+/- 0.02)	-	-

Tab. 1 : peaks assignment and their spin polarization.

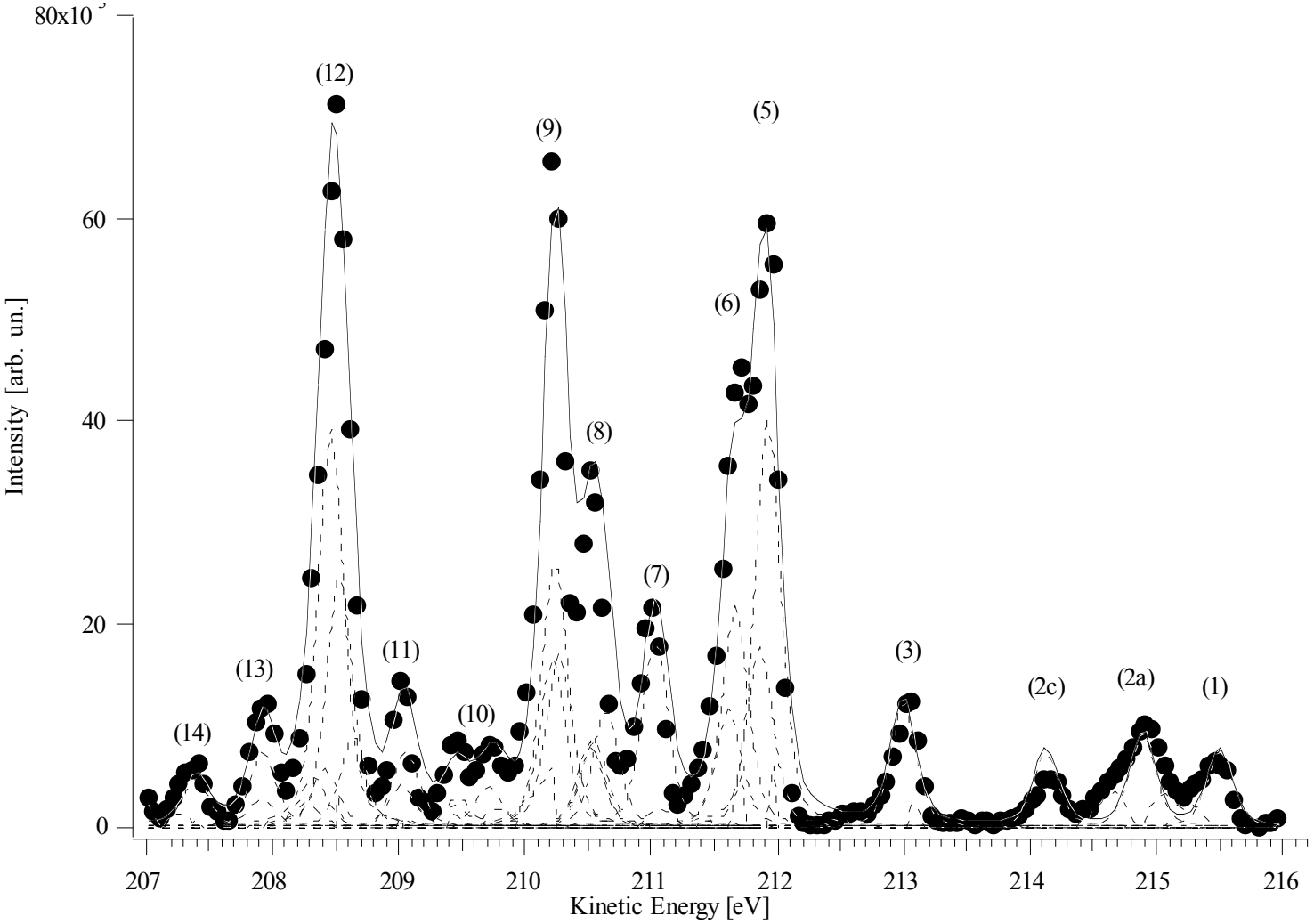

Fig. 1 : Ar $2p_{1/2}^{-1}$ 3d Auger decay, spin averaged. Circles : experimental. Full line: manifold. Dashed lines: manifold components (see text for details).

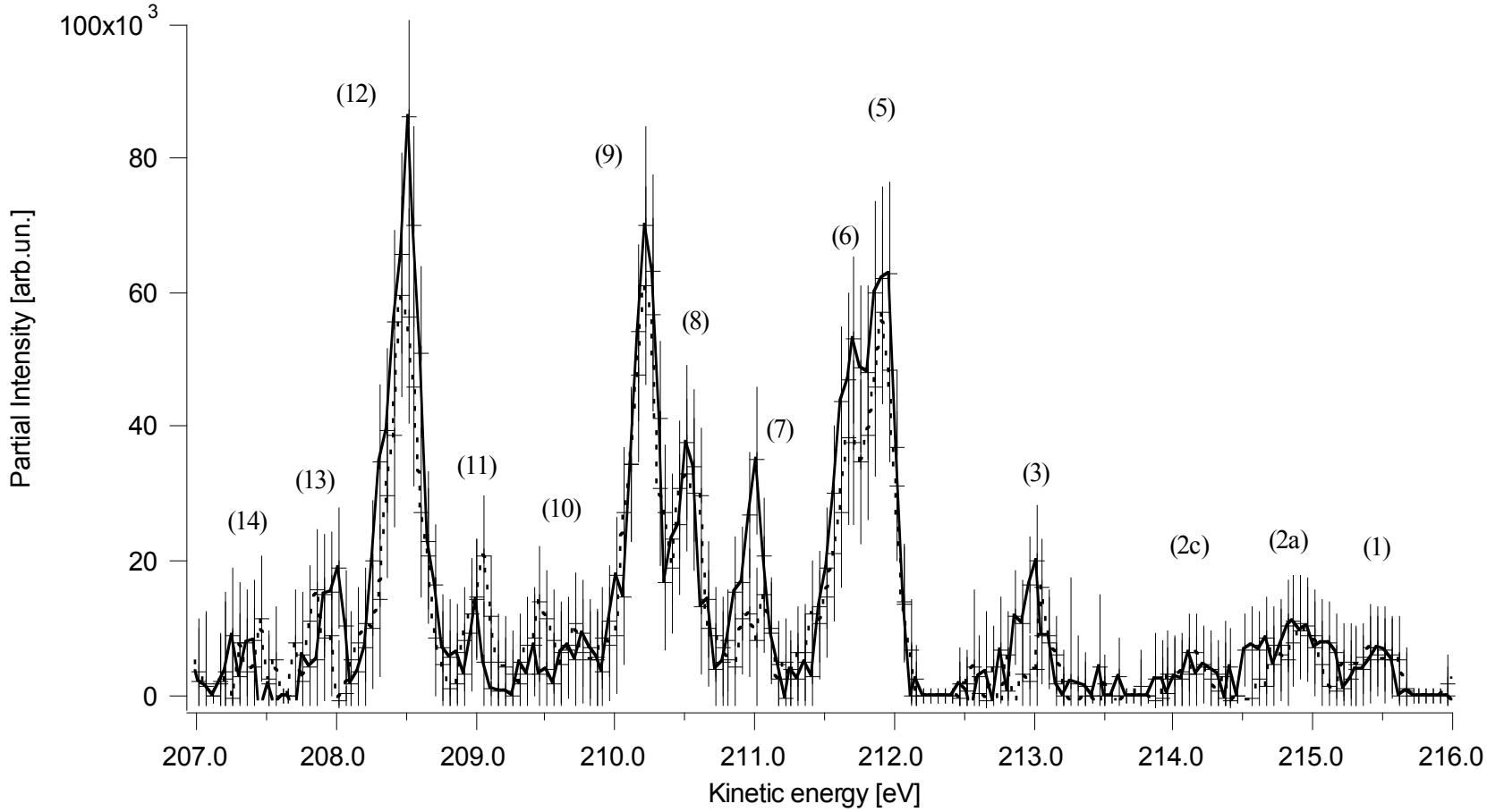

Fig. 2 : spin-resolved spectrum of Ar $2p_{1/2}3d$ Auger decay as measured with circularly polarized light. Full line: spin parallel, dashed line: spin anti-parallel, to photon propagation direction.

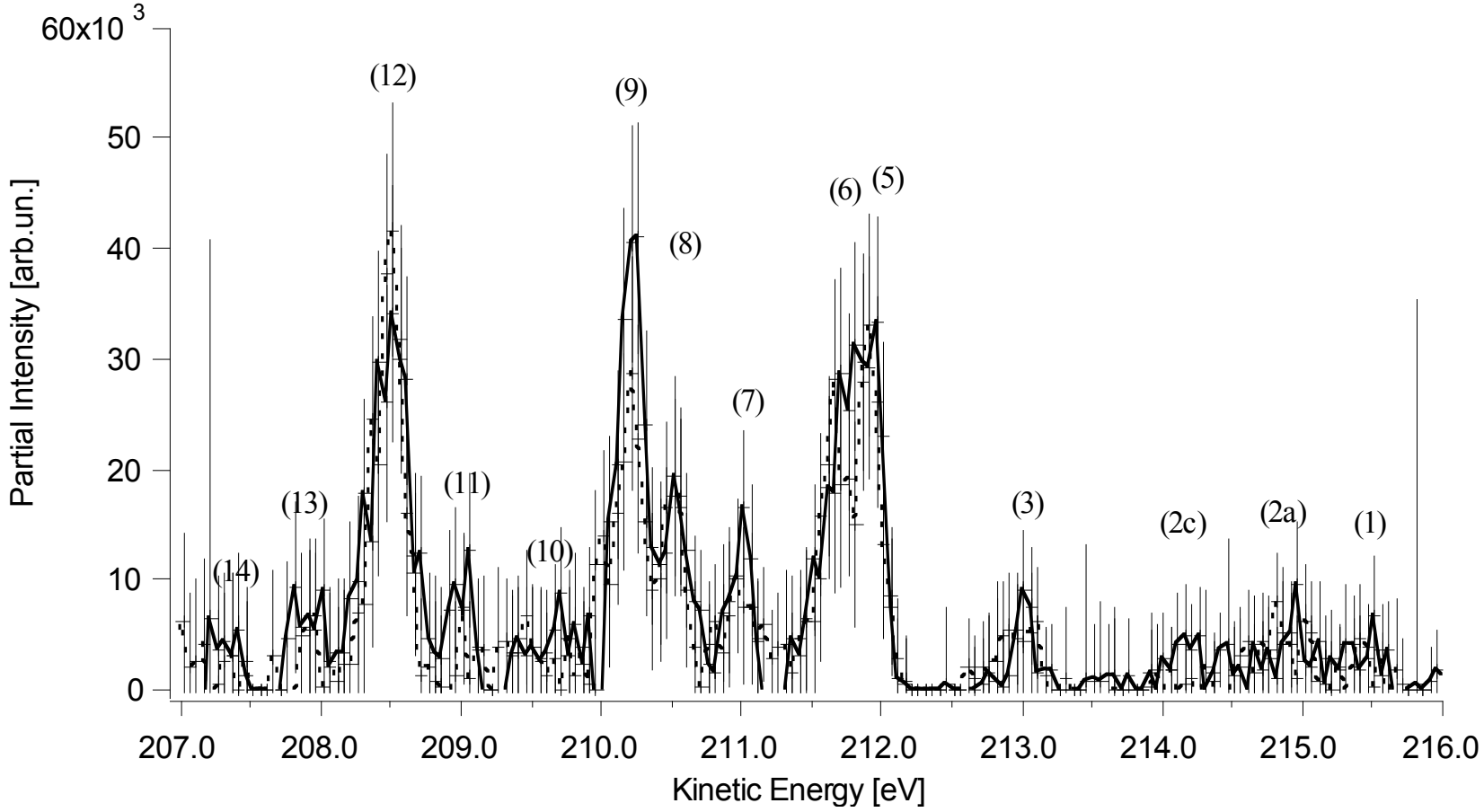

Fig.3 : same as fig.2 for linearly polarized light.

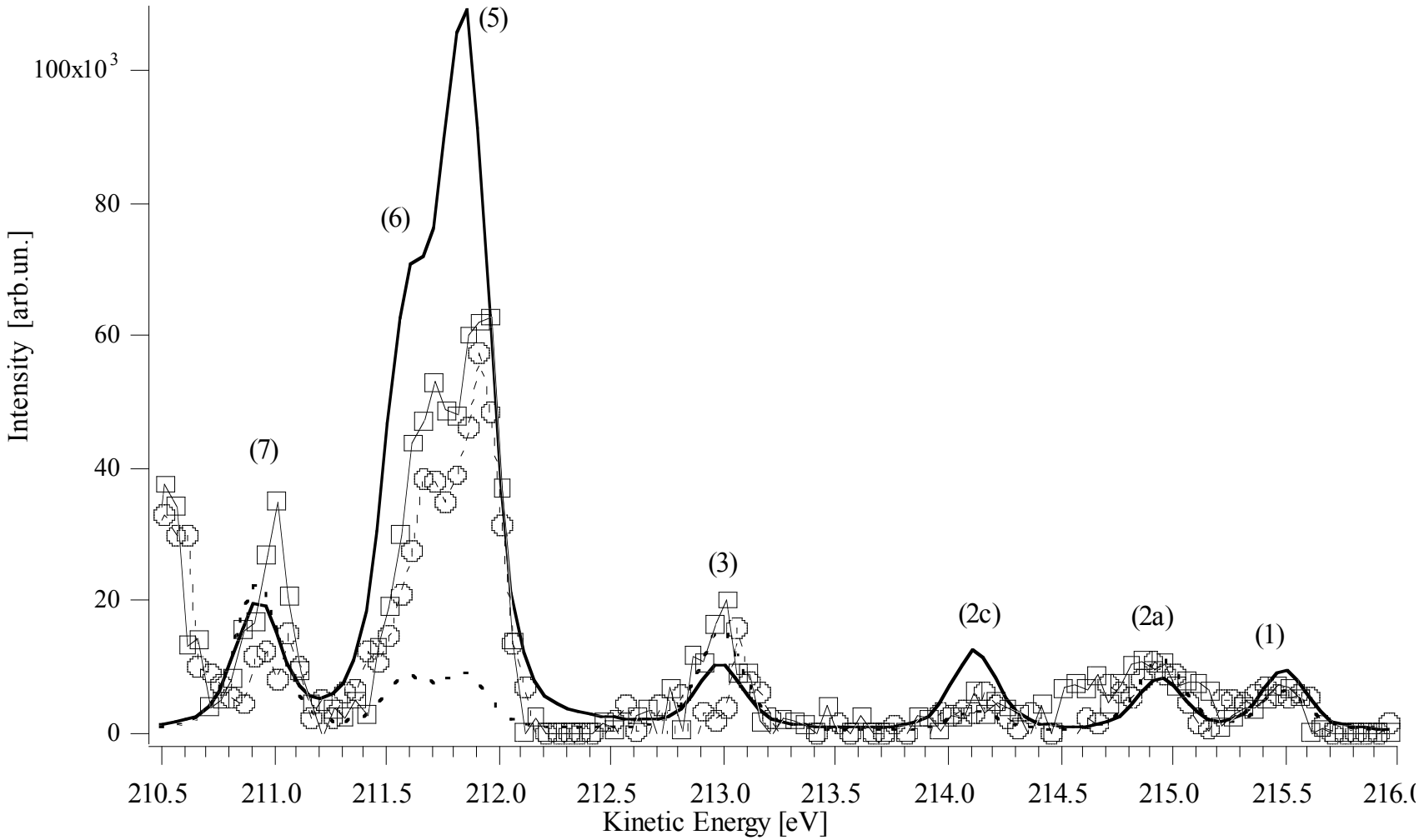

Fig. 4 : TSP of Ar $2p_{1/2}3d$ Auger decay, comparison with 36 CFS calculations. Experimental: □ spin parallel, ○ antiparallel. Calculations: Full line parallel, dashed line anti-parallel. Light lines are added to experimental data to guide the eye.

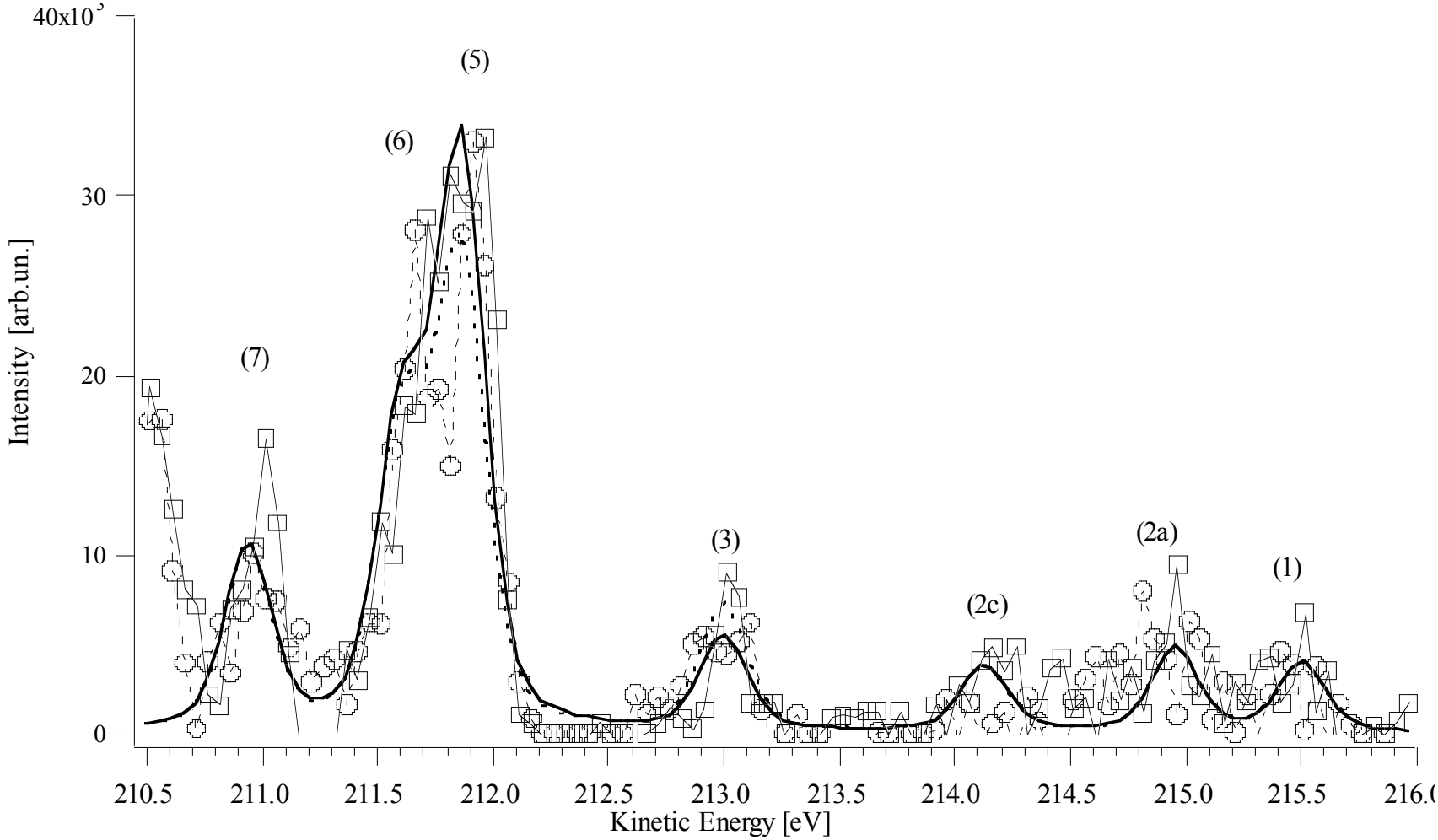

Fig. 5 : same as figure 4, for the DSP